Proton-induced coloring of multicomponent glasses

M. F. Bartusiak and J. Becher

Proton-induced absorption over the 280–700-nm region and growth of that coloring with increasing dosage of proton radiation were determined for three Schott glasses used as focusing elements in the International Ultraviolet Explorer. It was found that the absorption spectra for each glass can be fitted with three Gaussian shaped bands in the near UV–visible range, while a fourth Gaussian characterizes the absorption edge. For doses up to 10^7 rads, the dependence of the induced absorption α on total dose Φ is accurately described by the saturating exponential function $\alpha(\lambda,\Phi) = \alpha_s[1 - \exp(-b\Phi)]$, where α_s and b are constants dependent on the wavelength and glass type. The proton irradiation results were then compared to the effects of electron irradiation on those same three types of glass. For any one glass, it was determined that electrons and protons produced absorption bands with peaks at the same energies but with different saturation levels. For the glasses and wavelength region investigated, proton irradiation induced higher absorption saturation levels α_s in the longer wavelengths, while electron irradiation induced greater absorption in the shorter wavelengths.

Introduction

Meteorological satellites, orbiting astronomical telescopes, and exploratory spacecraft all carry with them complex optical systems whose transmission can be severely affected by the harsh radiation environment of space. Radiation-induced darkening of a spacecraft's refractive components can lower expected signal levels. Most investigations into this effect have used either electron or gamma-ray irradiation to simulate a space environment, mainly because of the easier accessibility of such sources for long-term studies. Detailed information on the coloring of glass by other types of radiation encountered in space, in particular protons, is limited. Yet there is a great need to examine proton-induced effects since solar flares, galactic cosmic radiation, and a large portion of the inner Van Allen belt radiation are composed of energetic protons and, depending on the orbit and the spacecraft's shielding, could be the main influence in degrading the transmission of a material. As a result of these concerns, the study described here was undertaken.

This paper will describe the coloring induced by 85-MeV protons in three Schott glasses representative of glass types used in space applications. They are now being used as focusing elements in the International Ultraviolet Explorer Fine Error Sensor. It will be shown that the absorption (i.e., coloring) induced in each glass by the radiation can be resolved into three optical absorption bands in the near UV–visible range. In addition, it will be discussed how that absorption grows with increasing dosages of protons, thus providing the means to predict degradation in any of the three glasses for a particular fluence of proton radiation. Similar analyses were performed on data obtained from a previous study on the effects of 7.0-MeV electron irradiation on those same three types of glass.[1] It will be shown that protons and electrons produce absorption bands with peaks at the same energies for any one glass but with different absorption saturation levels after irradiation to doses around 10^6 rads.

Mechanisms of Coloring

The mechanisms involved in the coloration of transparent crystals and glasses by radiation are fairly well understood.[2,3] Ionization is the dominant factor. In ionization, the incoming radiation detaches electrons from atoms of the material, allowing them to move through the atomic network. A few percent of these free electrons and resulting positive holes can be trapped in defects within the material, such as ion vacancies, impurities, or nonbridging oxygens. Once the charge carriers are trapped, they are capable of absorbing light by electronic transitions; the exact frequency will depend on the environment surrounding the trapped electron or hole. These optically active sites are the well-known color centers.

When this work was done both authors were with Old Dominion University, Physics Department, Norfolk, Virginia 23508; M. F. Bartusiak is now with Boston University, Physics Department, Boston, Massachusetts 02215.

Received 11 June 1979.
0003-6935/79/193342-05$00.50/0.

Table I. Characteristics of Schott Glasses[12]

Type	Abbe number[a] ν_d	Density (g/cm^3)	Index of refraction[b] n_d
LaK 21	60.10	3.74	1.641
KzFS N4	44.30	3.20	1.613
LF 5	40.85	3.22	1.581

[a] $\nu_d = (n_d - 1)/(n_F - n_C)$, where n_F is the index of refraction at the blue hydrogen line (486.1 nm) and where n_C is the index of refraction at the red hydrogen line (656.3 nm).

[b] n_d is the index of refraction at the yellow helium line (587.6 nm).

Two aspects of this radiation-induced coloring were examined. First, the absorption induced by the radiation was determined over the wavelength region of interest (i.e., an induced absorption spectrum).[4] To measure this, the total absorption before irradiation (a combination of the true absorption of the material and the apparent absorption due to reflectivity at the surface) was subtracted from the total absorption after irradiation. Since the apparent absorption is not appreciably affected by irradiation, surface reflection effects subtract out this way. The quantity that results is known as the induced absorption α. Second, it was seen how this induced absorption grows as a function of the total dose.

The induced absorption spectrum (with wavelength converted to its equivalent photon energy) consists of the superposition of Gaussian shaped absorption bands, each corresponding to a different color center.[5] Each absorption band at energy E can be described as

$$\alpha(E) = \alpha_m \exp\{-4 \ln 2[(E - E_0)/U]^2\}, \quad (1)$$

where E_0 is the photon energy in electron volts at the peak of the band, U is the full width at half-maximum, and α_m is the induced absorption at the band maximum. Growth of a radiation-induced absorption band in time at a constant flux has been found in investigations of alkali halides and glasses[6–9] to be described by one linear term and one or more saturating exponentials

$$\alpha(t) = \sum_{i=1}^{N} A_i[1 - \exp(-B_i t)] + \alpha_1 t, \quad (2)$$

where N is the number of exponential components, t is the time in seconds, A_i and B_i are the magnitude and growth constants, respectively, and α_1 is the slope of the linear component. Previous studies[10,11] have reported that one exponential component accurately describes radiation-induced absorption growth in a wide variety of glass types, particularly multicomponent Schott glasses.

In this investigation, the induced absorption was analyzed as a function of total dose Φ (in rads). Since Φ is related to time through the dose rate ϕ ($\Phi = \phi t$), Eq. (2) with $N = 1$ can be put into the alternate form

$$\alpha(\Phi) = \alpha_s[1 - \exp(-b\Phi)] + \alpha_L \Phi. \quad (3)$$

This result requires the assumption that coloring is independent of the dose rate ϕ, behavior generally found to be true in previous studies of radiation effects on glass.[10,11] The $\alpha_s[1 - \exp(-b\Phi)]$ term is usually viewed as representing the absorption that arises as the defects already present in the material become populated with holes and electrons. Because of their limited number (around 10^{15}–10^{17}/cm^3), these color centers saturate to a final level α_s. Higher dosages then create new defects which proceed to populate as the linear function $\alpha_L \Phi$.

Glasses and Experimental Procedure

The glass samples used in both the 85-MeV proton and 7.0-MeV electron irradiation experiments were procured from Schott Optical Glass, Incorporated (U.S.) and polished at the National Aeronautics and Space Administration's Goddard Space Flight Center. The samples were circular disks, 2.5 cm in diameter and 0.2 cm thick. Before irradiation, the glasses were transparent from the near UV (around 300 nm) to the near IR. The proton and electron ranges for each glass were much greater than the 0.2-cm thickness, thus providing a relatively uniform energy deposition throughout the sample. Three types of glass were irradiated. Using Schott nomenclature, these glasses are LaK 21 (lanthanum crown), KzFS N4 (special short flint), and LF 5 (light flint). Along with being used in space applications, they represent a wide variety of chemical composition, physical properties, and degradation effects due to irradiation (Table I).

The proton irradiations were carried out at the University of Maryland at College Park using an isochronous cyclotron. The samples were irradiated to cumulative fluences ranging from 5.0×10^{11} to 1.5×10^{14} protons/cm^2 in a scattering chamber evacuated to 10^{-6} Torr. The beam flux was between 10^{10} and 6×10^{11} protons/cm^2-sec. Determinations of flux and fluence were made with a Faraday cup and current integrator. After irradiation to a certain fluence, the samples were taken out of the chamber and their transmission spectra measured by a Perkin-Elmer model 200 spectrophotometer over the 280–700-nm wavelength region. Using peripheral interface equipment, the transmission measurements together with their corresponding wavelengths were monitored and stored using a DEC LSI-11 computer. The samples were then placed back into the chamber for further irradiation.

The electron irradiations were performed at the Space Radiations Effects Laboratory in Newport News, Virginia, using a linear electron accelerator. The glasses underwent cumulative fluences from 10^{11} to 10^{13} electrons/cm^2. A Faraday cup was used to determine the flux of each irradiation. Following each room-temperature irradiation, transmission measurements were made with a Cary-14 spectrophotometer in the 300–700-nm UV–visible region.

Transmission measurements during both the proton and electron experiments were taken approximately 1 h after irradiation. It is believed the bleaching, which occurs after irradiation, slowed sufficiently during the time that transient absorption effects decayed out, and only long-term absorption (i.e., absorption that is relatively stable at room temperature) remained.

Since ionization is the major factor in the coloration of glass, each fluence in particles/cm^2 has been converted to rads (1 rad = 100 ergs/g).[13] This measures the amount of energy that was transferred to the glasses by the incoming particle and often corresponds with the effects observed. While the conversions varied slightly depending on the density of each glass, they were ~1.2 $\times 10^7$ p/cm^2/rad for the 85-MeV protons and ~4.5 $\times 10^7$ e/cm^2/rad for the 7.0-MeV electrons.

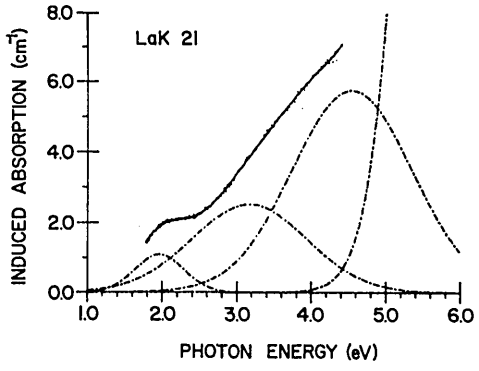

Fig. 1. The induced absorption spectrum of Schott LaK 21 after 85-MeV proton irradiation to a total dose of 3.0 $\times 10^5$ rads. The dashed lines indicate the resolution of the spectrum into a series of Gaussian shaped bands. The solid line through the data points is the sum of the individual bands.

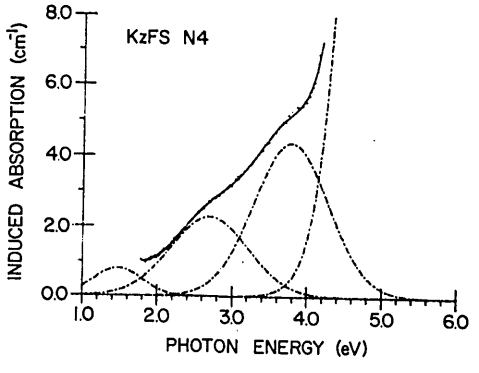

Fig. 2. The induced absorption spectrum of Schott KzFS N4 after 85-MeV proton irradiation to a total dose of 3.0 $\times 10^5$ rads.

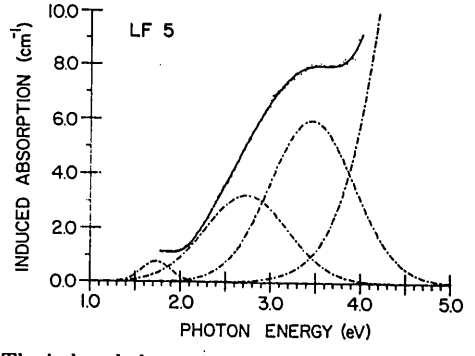

Fig. 3. The induced absorption spectrum of Schott LF 5 after 85-MeV proton irradiation to a total dose of 2.9 $\times 10^5$ rads.

Induced Absorption Spectra

Examples of absorption spectra induced by proton irradiation of the three glasses under study are shown in Figs. 1, 2, and 3. The spectra were resolved into a series of Gaussian shaped bands using a computer program that performed a least-squares fit to a nonlinear function,[14] in this case a sum of Gaussians [each Gaussian being defined by Eq. (1)]. The solid line through the data points in each figure is the sum of the individual absorption bands (dashed lines). By inspection it can be seen that the data were fitted very accurately. All the glasses exhibited three Gaussian bands in the near UV–visible region. However, each glass had its own unique fingerprint of band energies and halfwidths. All the resolved spectra also had a fourth Gaussian located with an absorption peak fitted at 5.5 eV or above. This high energy band can be regarded as the shift in the absorption edge toward longer wavelengths as the irradiation dosage increases.

The electron-induced absorption spectra for each glass showed the same band structure as their proton-induced counterparts. As an example, in Fig. 4, it can be seen that 7.0-MeV electrons produced absorption bands in LF 5 with peaks located at the same energies as the proton-induced bands (Fig. 3). This was also true for LaK 21 and KzFS N4. The band parameters obtained from the fitting process are given in Table II. All spectra measured for each glass after the various doses could be resolved into these bands.

Where absorption bands will be located in any particular glass is dependent on a number of variables, which include whether the glass was made under reducing or oxidizing conditions, the types and amounts of impurities in the glass, and the concentration of network modifying oxides in the material.[15] Since the composition of Schott glass is proprietary information, it is beyond the scope of this study to attribute each center to a particular kind of charge carrier trap. However, other studies of multicomponent glasses have found that most color centers in the visible region can be attributed to hole-trapping.[15]

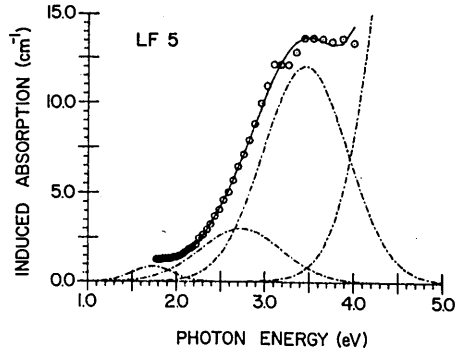

Fig. 4. The induced absorption spectrum of Schott LF 5 after 7.0-MeV electron irradiation to a total dose of 1.2 $\times 10^5$ rads. Note that the bands are located at the same energies as the LF 5 proton-induced absorption spectrum. This was true for LaK 21 and KzFS N4 as well. However, there are minor differences in the band halfwidths generated by each type of radiation.

Table II. Absorption Spectra Components: Band Energies and Halfwidths

Type of irradiation	Glass	Band energy E_0 (eV)	Halfwidth U (eV)
85-MeV protons	LaK 21	2.0	0.76
		3.2	1.8
		4.6	1.9
	KzFS N4	1.5	0.76
		2.7	1.2
		3.8	1.2
	LF 5	1.7	0.38
		2.7	1.1
		3.5	1.1
7.0-MeV electrons	LaK 21	2.0	0.80
		3.2	1.9
		4.6	1.9
	KzFS N4	1.5	0.8
		2.7	1.1
		3.8	1.4
	LF 5	1.7	0.55
		2.7	1.1
		3.5	1.1

Table III. Absorption Growth Parameters

Type of irradiation	Glass	λ (nm)	α_s (cm^{-1})	b (rad^{-1})
85-MeV protons	LaK 21	300	18	1.6×10^{-6}
		400	12	1.2×10^{-6}
		500	7.8	9.5×10^{-7}
		700	5.6	9.7×10^{-7}
	KzFS N4	400	11	1.3×10^{-6}
		500	6.4	1.3×10^{-6}
		700	3.4	8.8×10^{-7}
	LF 5	350	15	2.5×10^{-6}
		500	9.2	1.4×10^{-6}
		700	3.5	1.0×10^{-6}
7.0-MeV electrons	LaK 21	300	29	3.1×10^{-6}
		400	9.7	5.4×10^{-6}
		500	5.4	5.9×10^{-6}
		700	3.1	6.7×10^{-6}
	KzFS N4	400	17	2.4×10^{-6}
		500	6.7	3.8×10^{-6}
		700	2.5	4.8×10^{-6}
	LF 5	350	51	2.5×10^{-6}
		500	9.8	4.1×10^{-6}
		700	2.2	6.4×10^{-6}

Induced Absorption Growth Curves

As noted earlier, growth of induced absorption in any one band with increasing dose of irradiation has been accurately described in previous studies by Eq. (3). However, when an absorption spectrum consists of bands reasonably separated (as is the case in this investigation), Eq. (3) can also be used to describe the growth of the total induced absorption at a particular wavelength λ. For spectra which meet this condition, this simplifies the equation's use in practical applications. It has been reported that the $\alpha_L\Phi$ term can be set to zero since its contribution is negligible in the dose range under consideration ($\leq 10^7$ rads).[16] Thus, data obtained from both proton and electron irradiations of the glasses were fitted to the expression

$$\alpha(\lambda,\Phi) = \alpha_s[1 - \exp(-b\Phi)], \quad (4)$$

using a least-squares procedure. Constants α_s and b are dependent on λ and glass type. Their values were calculated at selected wavelengths, which spanned the entire spectrum under investigation. Some results for each glass are listed in Table III.

It can be seen from Table III that, while α_s changed rapidly with decreasing wavelength in all three glasses, the growth constant b remained relatively stable. For any one glass, b changed by no more than a factor of 2–3 for both the proton- and electron-generated growth curves. All the glasses had values for b falling in the same range (i.e., around 1.2×10^{-6} rad^{-1} for the proton-induced degradation data and about 5.0×10^{-6} rad^{-1} for the electron-induced degradation data). This behavior is consistent with previous findings on Schott glass[16] and provides a means for making rough estimations of the radiation-induced coloring of similar glass types.

Several absorption growth curves for LaK 21 after proton irradiation are shown in Fig. 5. Such curves typify the responses of all three glasses after either proton or electron irradiation. The solid line through the data points was computed using the constants α_s and b from the fitting process and indicates that Eq. (4) reasonably describes the growth of induced absorption at the selected wavelengths. The growth proceeded linearly on a log scale at the lower doses and then quickly attained a saturation level for a dose of around 10^6 rads. This same behavior has been reported in other types of electron-irradiated Schott glass.[11]

Comparison of Proton- and Electron-Induced Coloring

It has been shown that proton irradiation of the three glasses produced absorption bands with peaks at the same energies as those produced by electron irradiation. This agrees with the current model of coloration, which views the energies of color centers as being dependent on the glass, its defects, and composition. It was also shown that protons and electrons induced the same type of absorption growth with increasing dose. For doses up to 10^7 rads, the induced absorption α at wavelength λ exhibited a saturating exponential growth, thus providing the means to predict degradation in any of the three glasses for a particular fluence of proton or electron irradiation. However, the protons and electrons did not induce the same saturation levels α_s in any one

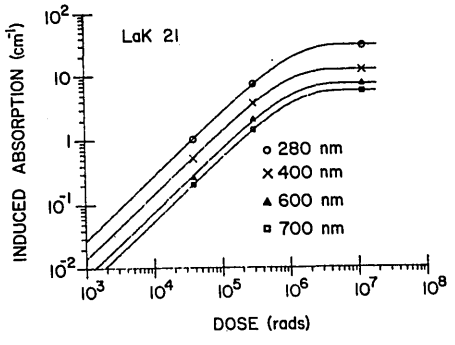

Fig. 5. The growth of induced absorption for Schott LaK 21 with an increasing dose of 85-MeV protons at selected wavelengths. All the glasses exhibited this saturating exponential growth during both the proton and electron irradiations for doses up to 10^7 rads.

glass for certain areas of the spectrum. In fact, a pattern is discerned as one compares the values of α_s in Table III. While the protons produced a higher absorption saturation level than the electrons at the longer wavelengths (around 700 nm), the reverse occurred in the shorter wavelengths (around 300 nm). In that area of the spectrum, the electrons induced a greater absorption.

The differences are not extreme at either end of the 280–700-nm spectrum, yet they are still larger than the fitted standard deviations (0.1–4%) of the saturating levels. For the three glasses tested, this indicates that the protons formed more low energy color centers at the saturation level than the electrons, while the electrons created a greater number of stable centers at the higher energies (at least for the range of energies being investigated). Should this finding hold for other glass types as well, it suggests that one must be careful in taking degradation effects produced by one type of charged particle and extrapolating effects produced by another type of radiation.

The authors express sincere thanks to W. Fowler and C. Reft for their help in the data acquisition and to L. C. Smith for assistance in the data analysis and computer graphing. This work has been supported by NASA grant NSG-5053.

References

1. J. Becher, C. S. Reft, and R. L. Kernell, "Radiation Studies of Optical and Electronic Components Used in Astronomical Satellite Studies," Old Dominion University Technical Report PGSTR-PH77-55 (1977).
2. E. Lell, N. Kreidl, and J. R. Hensler, in *Progress in Ceramic Science, Vol. 4,* J. E. Burke, Ed. (Pergamon, Oxford, 1966).
3. R. A. Wullaert *et al.,* in *Effects of Radiation on Materials and Components,* J. F. Kircher and R. E. Bowman, Eds. (Reinhold, New York, 1964).
4. As used in this paper, an absorption k is defined by Lambert's law $I = I_0 \exp(-kx)$, where I_0 is the light intensity entering the material, and I is the intensity after passage through a thickness x. Transmission T is defined as I/I_0.
5. P. W. Levy, J. Am. Ceram. Soc. **43,** 389 (1960).
6. K. Lengweiler, P. L. Mattern, and P. W. Levy, Phys. Rev. Lett. **26,** 1375 (1971).
7. P. W. Levy, P. L. Mattern, and K. Lengweiler, Phys. Rev. Lett. **24,** 13 (1970).
8. P. W. Levy *et al.,* J. Am. Ceram. Soc. **57,** 176 (1974).
9. P. L. Mattern, K. Lengweiler, and P. W. Levy, Solid State Commun. **9,** 935 (1971).
10. M. Goldberg *et al.,* Nucl. Instrum. Methods **108,** 119 (1973).
11. M. J. Treadaway, B. C. Passenheim, and B. D. Kitterer, "Transient Radiation Effects in Optical Materials," SAMSO-TR-75-174 (1975).
12. Schott Optical Glass catalog.
13. With the absorbed dose nearly uniform throughout the material, the fluence is converted to rads through the following equation: Dose = $1/\rho\ \Phi\ dE/dt \cdot 1.6 \times 10^8$ rads, where ρ is the density of the irradiated material in g/cm^3, Φ is the fluence in particles/cm^2, and dE/dt is the particle's stopping power in MeV/cm.
14. P. R. Bevington, *Data Reduction and Error Analysis for the Physical Sciences* (McGraw-Hill, New York, 1969).
15. A. Bishay, J. Non-Cryst. Solids **3,** 54 (1970).
16. M. J. Treadaway, B. C. Passenheim, and B. D. Kitterer, IEEE Trans. Nucl. Sci. **NS-22,** 2253 (1975).

Patents *continued from page 3341*

An ophthalmic lens surfacing tool is provided with pyramidal mating protrusions that maintain accuracy of centering and rotational alignment of the tool and holder during wear in an abrasive environment. B.J.H.

4,148,548 10 Apr. 1979 (Cl. 350–1.3)

Temperature compensating focusing in infrared zoom lenses.

G. V. THOMPSON. Assigned to Pilkington P. E., Ltd. Filed 19 Sept. 1977 (in U.K. 2 Oct. 1976).

The lens has a front part and a rear part which are adjustable axially and a middle part which provides the variable focal length capability. The front part basically is for focusing. The positions of the front and rear parts relative to each other and to the middle part can be iteratively changed to provide a substantially focused image throughout the zoom range when the lens is at a required operational temperature different from the design temperature. The temperature coefficient of index of refraction is in general higher for IR materials. B.J.H.

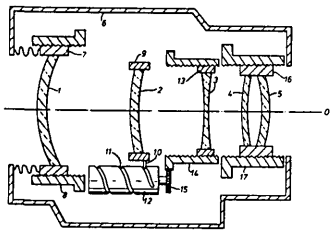

4,148,549 10 Apr. 1979 (Cl. 350–3.70)

Diffraction gratings.

A. TERMANIS. Assigned to The Rank Organisation, Ltd. Filed 8 Dec. 1976 (in U.K. 8 Dec. 1975).

Crossing beams from a laser harden a photoresist internally to provide planes that become the facets of a blazed diffraction grating. Much consideration is given to optical noise fringes so a rotating diffuser is required. C.F.M.

4,148,552 10 Apr. 1979 (Cl. 350–87)

Microscope adaptable to various observing methods.

H. SUZUKI and M. SHIO. Assigned to Nippon Kogaku K. K. Filed 26 Oct. 1976 (in Japan 28 Oct. 1975).

A versatile microscope structure is described which has three interchangeable light sources attached removably to aid operating through the hollow supporting structure. A variety of arrangements can be effected to permit use with a bright or dark field, fluorescence, polarization, etc. J.J.J.S.

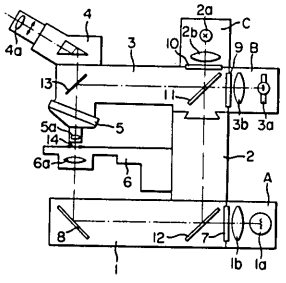

4,148,553 10 Apr. 1979 (Cl. 350–96.21)

Multifiber cable splicer.

A. R. ASAM. Assigned to International Telephone & Telegraph Corp. Filed 22 Nov. 1976.

A connector for joining one or more pairs of optical fibers uses a glass connector of triangular cross section to align the fibers precisely. One embodiment consists of a glass sleeve which is softened and crimped after the fibers are inserted. G.W.C.